Time-reversal invariance and universality of two-dimensional growth models

M. Plischke, Z. Rácz,* and D. Liu
Department of Physics, Simon Fraser University, Burnaby, British Columbia, Canada V5A 1S6
(Received 4 August 1986)

We study a model of interface dynamics which describes a surface-tension-biased process of simultaneous deposition and evaporation of particles. The control parameter of the model is the average translational velocity (v) of the interface which is determined by the difference between the rates of deposition and evaporation. For $v=0$ the dynamics is reversible and the two-dimensional problem can be solved exactly by mapping the system onto a kinetic Ising model. For the case of irreversible growth ($v\neq 0$), we use Monte Carlo methods to calculate the dynamic structure factor, $S(k,t)$, of the surface. We find that $S(k,t)$ obeys dynamic scaling: $S(k,t)\sim k^{-2+\eta}f(k^z t)$ with $\eta=0$ for all v, whereas $z=2$ for $v=0$ and $z=\frac{3}{2}$ for $v\neq 0$. These results suggest that the long-wavelength, long-time limit of our interface model can be described by Burgers' equation and, furthermore, that the change in the dynamical exponent z is related to the breaking of time-reversal symmetry which occurs as v becomes nonzero.

I. INTRODUCTION

A number of interesting phenomena can be described in terms of the motion of an interface between two phases of matter. Crystal growth, dielectric breakdown, fluid displacement in porous media, and electrodeposition are a few examples which are important from both the theoretical and practical point of view.[1–3] Although the equations describing these processes are well defined, theoretical advance is hampered by the fact that the surfaces are highly convoluted, display large fluctuations, and, as a consequence, even the question of how to characterize them (i.e., what to calculate) is largely open.

Since the clusters formed by interface evolution are often scale invariant, and since the large fluctuations in surface configurations are reminiscent of critical fluctuations in equilibrium systems, it is natural to try to characterize the surface by means of critical exponents, i.e., by the scaling dimensions of various macroscopic quantities. For complicated processes such as diffusion limited aggregation[4] one needs an infinite number of scaling dimensions[5] in order to describe the active zone of the surface[6] through the highly singular growth-probability measure.[7,8]

There are less singular surface-evolution models, however, such as the Eden process[9] or the ballistic deposition model.[10] They seem to be describable in terms of simpler quantities such as the width of the active zone, and Monte Carlo simulations[11–13] indicate that two exponents are sufficient to characterize these growth processes.

The appearance of two exponents may be explained as follows. We let the growth process take place in a restricted geometry, for example in a strip in dimension $d=2$. The long-time limit of the surface evolution in this case is a stationary process. If one assumes that the steady-state fluctuations are in some sense analogous to equilibrium fluctuations one naturally arrives at the following two exponents. The static critical exponent η determines the scaling of time-independent quantities (e.g., the width of the active zone, ξ, is proportional to the magnitude of fluctuations in the surface position, and consequently scales with the linear size of the system, L, as $\xi\sim L^{(3-d-\eta)/2}$). The dynamic critical exponent, z, on the other hand, specifies the scaling of the characteristic time scale which might be taken to be the relaxation time of steady-state fluctuations ($\tau\sim L^z$).

If the analogy with equilibrium critical phenomena is sound, then η and z are universal, i.e., they depend only on such general features of the system as the dimensionality, the symmetries of the steady state, and the symmetries of the equation of motion. Thus one might try to classify simple growth processes according to the values of η and z, and, furthermore, these exponents may be calculated from highly idealized field theoretic models which retain only the relevant features of the growth process.

A significant development in the above program has been the recent introduction of a field theoretic model of deposition by Kardar *et al.*[14] Their model is an improvement over an earlier theory[15] which already contains the essential features of the deposition process—smoothing by surface tension and the effect of the average translation of the surface. Edwards and Wilkinson,[15] however, used a linearization procedure and, as a consequence, the effect of the uniform motion was lost. The relative surface fluctuations became independent of the velocity of the average translation. Kardar *et al.*[14] realized that the average translation affects the surface fluctuations significantly and included in the equation of motion the simplest nonlinear term which might be produced by the uniform motion of the surface. The result is Burger's equation[16] which has been analyzed by renormalization group methods.[14,17] The average translation is indeed found to be a relevant perturbation; without it (equilibrium case) the critical exponents take on their "free-field" values,[15] $\eta=0$ and $z=2$, while $\eta=0$ and $z=\frac{3}{2}$ in the nonequilibrium case of a surface advancing with an arbitrary nonzero velocity. Monte Carlo simulations of both the ballistic deposition model[11,18] and the Eden process[13] yield $\eta\approx 0$

and $z \approx 1.5$ indicating that Burgers's equation may be a prototype equation for describing the long-wavelength and low-frequency properties of a large class of growth models.

In order to study the extent of the universality class of Burgers's equation and to investigate the effects of a moving interface, we introduce in this paper (Sec. II) a simple growth model which contains the average translational velocity (v) as a parameter. In the equilibrium case ($v=0$) the growth algorithm is microscopically time-reversible and an exact solution (Sec. III) leads to $\eta=0$ and $z=2$ which characterize the unstable fixed point[14] of Burger's equation. When $v\neq 0$ and time-reversal symmetry is broken we find by Monte Carlo simulations (Sec. IV) that the exponents ($\eta=0$, $z=\frac{3}{2}$) of the nontrivial fixed point of the Burgers's equation describe the evolution of the interface. The change of z from 2 to $\frac{3}{2}$ can thus be interpreted as being due to the breaking of time-reversal symmetry. Since various values of v can be studied we also observe crossover between the two types of behavior. Finally, on the basis of Monte Carlo simulations of a second simple model (Sec. V) we present further evidence that the origin of the change in the critical exponent z may be the breaking of time-reversal symmetry.

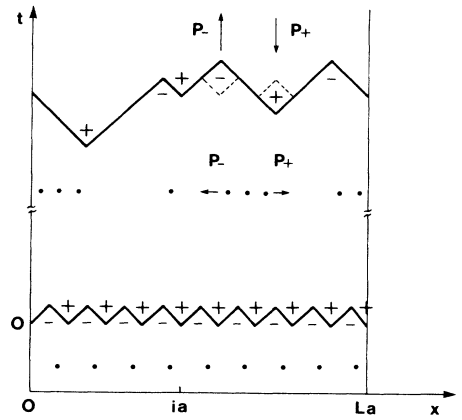

FIG. 1. Model I of deposition-evaporation governed interface evolution. The sites at which deposition (evaporation) occurs at a rate proportional to p_+ ($p_-=1-p_+$) are denoted by $+$ ($-$). The $t=0$ state is a "flat" substrate. The equivalent lattice gas model which is obtained by replacing every surface element of slope -1 with a hard-core particle is also shown.

II. A MODEL OF INTERFACE DYNAMICS (MODEL I)

The model of interface dynamics which we study is designed to mimic some of the essentials of simple deposition processes such as near-equilibrium crystal growth and the Eden process. The two elementary steps—deposition and evaporation—which define the surface evolution are illustrated in Fig. 1 for the particular case of the square lattice. Although we shall be working with this lattice throughout this paper, generalization to other lattices and higher dimension should be obvious from the construction.

As one can see from Fig. 1, the particles in this model are squares with sides of length $\sqrt{2}a$. The motion of the surface is restricted to an infinite strip in the [1,1] direction of the square lattice. The width of the strip is aL and periodic boundary conditions are employed in the direction perpendicular to the strip.

Time is discretized $t=t_n=n\tau$ and in a unit of time τ either a new particle is deposited at one of the local minima of the surface or a particle evaporates from one of the local maxima. The probability of deposition and evaporation are p_+ and $p_-=1-p_+$, respectively, and the place where the event occurs is chosen randomly from the available sites. As an initial condition we use a "flat" substrate as shown in Fig. 1.

Further motivation for introducing the above model comes from the observation that the density fluctuations in a one-dimensional hard-core lattice gas are described[19] on a coarse time and length scale by Burgers's equation. Kardar *et al.*,[14] on the other hand, arrived at Burgers's equation when studying the dynamics of the coarse-grained slope of a moving interface. Thus, identifying the density of the lattice gas with the slope of the interface we see the equivalence of the two systems on a coarse-grained level. The equivalence can be brought down to the microscopic level by considering the lattice gas model with half the sites occupied and identifying occupied and unoccupied sites with surface elements of slope -1 and $+1$, respectively (see Fig. 1). To complete the identification, the deposition and evaporation rates (p_+ and p_-) must be equated to the rates with which the particles hop to the right and left, respectively.

The advantage of introducing this "discrete-slope" surface model is that a two-state variable is associated with every lattice site and the system can thus be treated as a kinetic Ising model and, as a consequence, analytic results can be obtained at least for the case of $p_+=\frac{1}{2}$ (Sec. III).

We note here that recently Meakin *et al.*[18] have arrived at the $p_+=1$ limit of the above model by a different route. They studied the ballistic deposition model[10] and noted that on the average the height difference of neighboring columns was of the order of 1 lattice site. It was then a natural simplification to restrict the height difference to ± 1 and to treat the system as a spin model.

Returning to the properties of the surface formed in the process defined above we note that the surface can be described by the single valued function h_j which is the height of the surface measured from a reference level at sites $x_j=ja$, $j=1,2,\ldots,L$. Once the time evolution of $h_j(t_n)$ is measured in a Monte Carlo simulation or calculated analytically, various macroscopic characteristics of the surface can be obtained. A trivial quantity is the average surface height which is given by

$$\langle h(t_n)\rangle=\frac{1}{L}\sum_{i=1}^{L}\langle h_i(t_n)\rangle=(2p_+-1)\frac{2a}{\tau}t_n\ , \qquad (1)$$

where we have chosen the average height of the initial state as the reference level. The averages $\langle\ \rangle$ in (1) are over the normalized distribution function $P(\{h\},t_n)$

which gives the probability that a configuration $\{h\}=\{h_1,h_2,\ldots,h_L\}$ occurs at time t_n. It is clear from (1) that unless $p_+=\frac{1}{2}$, which we shall call the equilibrium case, the surface moves on the average with a nonzero velocity. In order to characterize the intrinsic fluctuations in the co-moving frame one can consider the width of the surface zone, ξ, defined as

$$\xi^2(L,t)=\frac{1}{L}\sum_{j=1}^{L}\langle[h_j(t)-\langle h(t)\rangle]^2\rangle \ . \tag{2}$$

More detailed information about the surface structure may be obtained by calculating the time-dependent structure factor

$$S(k,t)=\langle\hat{h}_k(t)\hat{h}_{-k}(t)\rangle \ , \tag{3}$$

where

$$\hat{h}_k(t)=\frac{1}{\sqrt{L}}\sum_{j=1}^{L}(h_j(t)-\langle h(t)\rangle)e^{ikj} \tag{4}$$

with $k=2n\pi/L$, $n=0,\pm1,\pm2,\ldots,\pm(L/2-1),L/2$.

In the long-time limit the evolution of the surface is expected to become a stationary process and $\xi^2(L,t)$ and $S(k,t)$ become time independent. The relaxation toward this stationary state may be characterized by the time correlations in the stationary state

$$\Phi(k,t)=\lim_{t'\to\infty}\frac{1}{S(k,t)}\langle\hat{h}_k(t+t')\hat{h}_{-k}(t')\rangle \ , \tag{5}$$

which describes the dynamics of near-stationary-state processes. The far-from-stationary-state dynamics, on the other hand, can be investigated by using the relaxation function:

$$\Psi(k,t)=\frac{S(k,\infty)-S(k,t)}{S(k,\infty)-S(k,0)} \ . \tag{6}$$

Since, in this model, there is no mechanism which restricts the long-wavelength fluctuations, one expects that the fluctuations diverge ($\xi\to\infty$) in the limit $L\to\infty$, and this limit may be considered a critical point of the system. Consequently, for large enough L, one anticipates a dynamic scaling form for the functions (3), (5), and (6), i.e., the long-wavelength long-time limit of the structure factor, for example, may be analyzed in terms prescribed by dynamic scaling theory for finite-size systems:

$$S(k,t)\sim k^{-2+\eta}f(k^z t,kL) \ , \tag{7}$$

where the static (η) and dynamic (z) exponents determine the universality class the model belongs to. The results of Monte Carlo simulations presented in Sec. IV confirm these expectations. Before turning to the simulations, however, we show that the equilibrium limit ($p_+=\frac{1}{2}$) can be solved exactly with the result $\eta=0$ and $z=2$ and, furthermore, present arguments which suggest that the $p_+\neq\frac{1}{2}$ case is in one universality class with the field theoretic interface model studied by Kardar *et al.*[14]

In order to derive analytical results it is convenient to work with the continuous time version of our model which is defined through the following master equation:

$$\frac{\partial P(\{h\},t)}{\partial t}=-\sum_{i=1}^{L}w_i(\{h\})P(\{h\},t)+\sum_{i=1}^{L}w_i(\{h\}_i)P(\{h\}_i,t) \ . \tag{8}$$

Here $w_i(\{h\})$ is the rate of deposition or evaporation at site i:

$$w_i(\{h\})=\begin{cases}p_+/\tau_0, & \text{if site } i \text{ is a local minimum} \ ,\\ (1-p_+)/\tau_0, & \text{if site } i \text{ is a local maximum} \ ,\\ 0, & \text{otherwise} \ .\end{cases} \tag{9}$$

In Eq. (9) τ_0 is a parameter which sets the time scale and the configurations $\{h\}_i$ in (8) differ from $\{h\}$ by the addition or removal of a particle at site i provided that the configuration $\{h\}$ allows such a change in the surface.

Clearly, the discrete and continuous time versions of the model are identical in the sense that particles deposit or evaporate independently and at a rate proportional to p_+ and $1-p_+$, respectively. The time scales of the two models, however, are related in a nontrivial manner. If we call the deposition or evaporation of a particle an event and measure time in the number of these events then time flows uniformly in the discrete time model, $t_n=n\tau$, while the continuous-time version displays fluctuations in the time increments due to fluctuations in the number of local minima and maximum of the surface. The two times can be related, however, by equating the average number of events $\langle n(t)\rangle$ in the continuum version to n of the discrete model:

$$\langle n(t)\rangle=\int_0^t\sum_{i=1}^{L}\langle w_i\rangle dt=n=\frac{t_n}{\tau_0} \ , \tag{10}$$

thus yielding the required relationship $t_n=\varphi(t)$, provided that one can calculate $\langle w_i\rangle$. As we shall show in the next section, $\langle w_i\rangle$ and the various correlation functions of interest (3), (5), and (6) can be calculated analytically for the particular case of $p_+=\frac{1}{2}$ in the continuum model by mapping this system onto a kinetic Ising model.

III. ANALYTICAL RESULTS

The mapping of the continuous time interface dynamics onto a one-dimensional kinetic Ising model is based on the observation that the height difference, h_i-h_{i-1} between neighboring points on the surface can only be $+a$ or $-a$. Thus all the intrinsic properties of the surface may be described in terms of a set of Ising variables $\{\sigma\}=\{\sigma_1,\sigma_2,\ldots,\sigma_L;\sigma_{L+1}=\sigma_1\}$ where

$$\sigma_i=\frac{h_i-h_{i-1}}{a}=\pm1 \ . \tag{11}$$

The master equation (8) then becomes an equation for the probability distribution $P_I(\{\sigma\},t)$ of the Ising states:

$$\frac{\partial P_I(\{\sigma\},t)}{\partial t}=-\sum_i w_i^{(I)}(\{\sigma\})P_I(\{\sigma\},t)+\sum_i w_i^{(I)}(\{\sigma\}_i)P_I(\{\sigma\}_i,t) \ , \tag{12}$$

where the state $\{\sigma\}_i$ differs from $\{\sigma\}$ by flipping both σ_i and σ_{i+1} and the flip rate is given by

$$w_i^{(I)}(\{\sigma\})=\frac{1}{4\tau_0}[1-\sigma_i\sigma_{i+1}+\alpha(\sigma_{i+1}-\sigma_i)] \tag{13}$$

with $\alpha=2p_+-1$. One can easily see that $w_i^{(I)}$ is nonzero only if $\sigma_i\neq\sigma_{i+1}$, i.e., if there is a local minimum or maximum in the surface at site i. Furthermore, $w_i^{(I)}=p_+/\tau_0$ for the case of a minimum ($\sigma_i=-1$, $\sigma_{i+1}=+1$) while $w_i^{(I)}=(1-p_+)/\tau_0$ for a maximum ($\sigma_i=+1$, $\sigma_{i+1}=-1$) in agreement with (9). We note that these spin-flip processes conserve the total magnetization and that the periodic boundary conditions in the original model force the number of up and down spins to be equal.

The advantage of the spin formulation of the problem is that one can easily derive a closed set of differential equations for the two-point correlation functions:

$$\langle\sigma_j\sigma_m\rangle=\sum_{\{\sigma\}}\sigma_j\sigma_m P_I(\{\sigma\},t) \tag{14}$$

and the width of the surface region $\xi(L,t)$ and the structure factor $S(q,t)$ can be expressed in terms of $\langle\sigma_j\sigma_m\rangle$. Indeed, the deviation of the surface height from the average height at site i is given by

$$\delta h_j=h_j-\langle h\rangle=a\left[\sum_{m=1}^{i}\sigma_m-\frac{1}{L}\sum_{m=1}^{L}\sum_{i=1}^{m}\sigma_i\right] \tag{15}$$

and, consequently,

$$\xi^2(L,t)=\langle(\delta h_i)^2\rangle=\frac{a^2}{L^2}\sum_{i=1}^{L}\sum_{j=1}^{L}\sum_{m=1}^{i}\sum_{n=1}^{j}C_{m-n}(t)\ , \tag{16}$$

where we have assumed that the initial state is translationally invariant (e.g., the initial state shown in Fig. 1 and the same state shifted horizontally a distance a are mixed with equal probability) and thus $\langle\sigma_j\sigma_m\rangle$ can be written as $\langle\sigma_j\sigma_m\rangle=C_{j-m}(t)$. Furthermore, we have used the fact that $\sum_i\sigma_i=0$ yields the following identity for the correlation functions

$$1+\frac{2}{L}\sum_{m,j>1}\langle\sigma_j\sigma_m\rangle=0\ . \tag{17}$$

The equation for $C_m(t)$ can be derived by following Glauber's[20] method. Taking the time derivative of Eq. (14) and using the master equation (12), one finds, for $|j-m|\geq 2$:

$$2\tau_0\frac{\partial}{\partial t}\langle\sigma_j\sigma_m\rangle=-4\langle\sigma_j\sigma_m\rangle+\langle\sigma_{j+1}\sigma_m\rangle+\langle\sigma_{j-1}\sigma_m\rangle+\langle\sigma_j\sigma_{m+1}\rangle+\langle\sigma_j\sigma_{m-1}\rangle$$
$$-\alpha(\langle\sigma_{j-1}\sigma_j\sigma_m\rangle-\langle\sigma_j\sigma_m\sigma_{m+1}\rangle+\langle\sigma_j\sigma_{m-1}\sigma_m\rangle-\langle\sigma_j\sigma_{j+1}\sigma_m\rangle)\ , \tag{18a}$$

while the $m=j+1$ equation is given by

$$2\tau_0\frac{\partial}{\partial t}\langle\sigma_j\sigma_{j+1}\rangle=-2\langle\sigma_j\sigma_{j+1}\rangle+\langle\sigma_{j-1}\sigma_{j+1}\rangle+\langle\sigma_j\sigma_{j+2}\rangle-\alpha(\langle\sigma_{j-1}\sigma_j\sigma_{j+1}\rangle-\langle\sigma_j\sigma_{j+1}\sigma_{j+2}\rangle)\ . \tag{18b}$$

In the case of equilibrium growth ($\alpha=0$), Eqs. (18a) and (18b) contain only two-spin correlation functions and this makes the problem solvable as we shall show below. For $\alpha\neq 0$, the three-spin correlations appearing on the right-hand side do not, in general, cancel due to the lack of reflection symmetry in the kinetic Ising model [see Eq. (13)]. In turn, the lack of reflection symmetry can be traced back to the loss of time-reversal invariance for $\alpha=2p_+-1\neq 0$. A consequence of this symmetry breaking is that equations (18a) and (18b) couple to a hierarchy of equations for the many-spin correlation functions and we are unable to solve these equations exactly. We shall return to the problem of nonequilibrium growth in Sec. III B, but first the exactly solvable case of $\alpha=0$ will be discussed.

A. Equilibrium dynamics: $\alpha=0$

We assume a translationally invariant initial state. Equations (18a) and (18b) then reduce to a set of $L/2$ equations:

$$\tau_0\dot{C}_1=C_2-C_1\ ,$$
$$\tau_0\dot{C}_j=C_{j-1}-2C_j+C_{j+1},\quad \frac{L}{2}\geq j\geq 2\ . \tag{19}$$

The remaining correlation functions follow from the periodic boundary conditions: $C_{L/2+j}=C_{L/2-j}$. (We note that L must be even since $\sum_i\sigma_i=0$.) Actually, it is more convenient to consider (19) for $j=1,2,\ldots,L$ and to seek solutions which obey the aforementioned symmetry $C_{L/2+j}=C_{L/2-j}$. They are found by Fourier transformation of Eqs. (19), with the result:

$$C_j(t)=\frac{1}{L-1}\sum_q e^{iq(L/2-j)}C(q,0)\times\exp(-\lambda_q t/\tau_0)\ , \tag{20}$$

where the sum is over the following values of q

$$q=\frac{2\pi}{L-1}n,\quad n=0,\pm1,\pm2,\ldots,\pm(L/2-1) \tag{21}$$

and the relaxation rate per unit time is given by

$$\lambda_q=2[1-\cos(q)]\ . \tag{22}$$

Furthermore, $C(q,0)$ is the Fourier transform of the initial correlations $C_m(0)$. For the particular initial state shown in Fig. 1, $C(q,0)$ has the form

$$C(q,0)=-1/\cos(qL/2)\ . \tag{23}$$

After substituting (20) and (23) into (16), a tedious but straightforward calculation yields a simple expression for the width of the surface zone:

$$\frac{1}{a^2}\xi^2(L,t)=\frac{L+1}{12}-\frac{1}{L}\sum_{q\,(\neq 0)}\frac{1}{\lambda_q}\exp(-\lambda_q t/\tau_0)\ . \tag{24}$$

The result for the equilibrium ($t\to\infty$) width

$$\xi(L,\infty)=a\left[\frac{L+1}{12}\right]^{1/2} \tag{25}$$

indicates that the surface is rough. It is noteworthy that the result (25) can also be derived by simply assuming that the spins σ_i are $+1$ or -1 with independent and equal probabilities and subject only to the restriction that $\sum_i \sigma_i=0$. This similarity to free-field behavior is also seen in the time-independent piece of (24) which consists of independent modes decaying in a simple exponential fashion. The only difference from the discretized version of the free-field theory of deposition[15] is that the values of $q=2\pi n/(L-1)$ (Ref. 21) are slightly shifted from those expected for a system with periodicity L ($k=2\pi n/L$). This shift, however, is negligible in the limit $L\to\infty$ and, consequently, for large t, $\xi(L,t)$ obeys dynamics scaling following from the free-field theory:[15]

$$\xi(L,t)\approx L^{1/2}f(t/L^2)\ . \tag{26}$$

Since the structure factor $S(k,t)$ is related to ξ through

$$\xi^2(L,t)=\frac{1}{L}\sum_k S(k,t)\ , \tag{27}$$

Eq. (26) implies that the exponents η and z are equal to their classical values $\eta=0$, $z=2$, provided that the sum in (27) is dominated by the contribution from small k and $S(k,t)$ scales as given in Eq. (7). In fact, we do not need the above assumptions to find η and z since $S(k,t)$ can be calculated directly. We note, however, that $S(k,t)$ cannot be read off from the comparison of (27) and (24) because the sum in (27) is over $k=2\pi n/L$ while the values of q in (24) are shifted: $q=2\pi n/(L-1)$.

The simplest way of evaluating $S(k,t)$ is to Fourier transform (4) the identity

$$\begin{aligned}a^2C_m(t)&=a^2\langle\sigma_i\sigma_{i+m}\rangle\\&=2g_m(t)-g_{m-1}(t)-g_{m+1}(t)\ ,\end{aligned} \tag{28}$$

where

$$g_m(t)=\langle(h_j-\langle h\rangle)(h_{j+m}-\langle h\rangle)\rangle\ . \tag{29}$$

The right-hand side then becomes $\lambda_k S(k,t)$ while the left-hand side is determined by using the solution (20) for $C_m(t)$. The result for $k\neq 0$ is

$$\begin{aligned}\frac{1}{a^2}S(k,t)=&\frac{1}{(L-1)\lambda_k}\\&-\frac{1}{L-1}\sum_{q\,(\neq 0)}\frac{1}{\lambda_q-\lambda_k}\exp(-\lambda_q t/\tau_0)\ ,\end{aligned} \tag{30}$$

while the $k=0$ value, $S(0,t)=0$, follows from the identity $\sum_i(h_i-\langle h\rangle)=0$. We note that there are no singular terms in (30) since the possible values of k and q are never equal to each other.

In order to see the scaling of $S(k,t)$ we consider Eq. (30) for small k and large time or, more precisely, in the limit $kL=2\pi n$, $k^2t=m$ (n,m fixed) and $L\to\infty$. In this limit the sum in (30) is dominated by the $q=\pm q(n)=\pm 2\pi n/(L-1)$ terms since $\lambda_{q(n)}-\lambda_k\sim L^{-3}$ while $\lambda_q-\lambda_k\sim L^{-2}$ for other values of $q\sim L^{-1}$. (We note that there is an exponential cutoff in the contribution from larger q's because of the condition $k^2t=m$.) Separating the $q(n)$ terms and using $\lambda_k\approx k^2$, one can write

$$\begin{aligned}\frac{1}{a^2}S(k,t)=&\frac{1}{k^2}[1-\exp(-k^2t/\tau_0)]\\&+\frac{1}{k}Q(k^2t,kL)\ ,\end{aligned} \tag{31}$$

where the correction to scaling term $Q(k^2t,kL)/k$ may be obtained by transforming the remainder of the sum into a principal value integral and expanding expressions of the type $L/(L-1)$ in powers of L^{-1}. The correction is negligible in the scaling limit discussed above and, comparing (31) to (7), one can see that $\eta=0$ and $z=2$ as was suggested by the scaling form of $\xi(L,t)$.

B. Nonequilibrium growth: $\alpha\neq 0$

It would be of great interest to extend the above calculation to the case of the moving interface ($p_+\neq\frac{1}{2}$) and to see if the exponents η and z change their value. Unfortunately, the loss of time-reversal symmetry associated with the moving interface complicates the equations to a degree that we are unable to solve them. As suggested by the mapping of the interface model onto the driven hard-core lattice gas, however, one can relate the properties of the interface, at least in an approximate way, to the field theoretic model of Kardar *et al.*[14] To do this we shall focus on the average slope of the interface instead of the pair-correlation function.

An equation for the average slope

$$\left\langle\frac{1}{a}(h_i-h_{i-1})\right\rangle=\langle\sigma_i\rangle=\sum_{\{\sigma\}}\sigma_i P_I(\{\sigma\},t) \tag{32}$$

can be obtained by taking the time derivative of $\langle\sigma_i\rangle$ and using the master equation (12). The result is

$$\begin{aligned}2\tau_0\frac{\partial}{\partial t}\langle\sigma_i\rangle=&\langle\sigma_{i-1}\rangle-2\langle\sigma_i\rangle+\langle\sigma_{i+1}\rangle\\&+\alpha\langle\sigma_i(\sigma_{i+1}-\sigma_{i-1})\rangle\ .\end{aligned} \tag{33}$$

Some insight into the behavior of the model can now be gained by comparing (33) with Burgers's equation:

$$\frac{\partial v}{\partial t}=\nu\frac{\partial^2 v}{\partial x^2}+\lambda v\frac{\partial v}{\partial x}+\frac{\partial\eta}{\partial x} \tag{34}$$

which can be obtained[14] from a simple Langevin equation describing the evolution of the profile $h(x,t)$ of an interface:

$$\frac{\partial h}{\partial t}=\nu\frac{\partial^2 h}{\partial x^2}+\frac{\lambda}{2}\left[\frac{\partial h}{\partial x}\right]^2+\eta\ . \tag{35}$$

Here the term $\partial^2 h/\partial x^2$ accounts for the relaxation of the surface due to surface tension effects, $(\partial h/\partial x)^2$ is the simplest nonlinear term which can appear as a result of the uniform motion of the interface,[14] and $\eta(x,t)$ represents Gaussian white noise. The connection between (34) and (35) is through

$$v(x,t)=\frac{\partial h}{\partial x}\ , \tag{36}$$

i.e., Eq. (34) is for the slope of the interface, as is Eq. (33). The similarity between (33) and (34) can be made more transparent by averaging (34) over the noise

$$\frac{1}{\nu}\frac{\partial}{\partial t}\langle v\rangle_\eta=\frac{\partial^2}{\partial x^2}\langle v\rangle_\eta+\frac{\lambda}{\nu}\left\langle v\frac{\partial v}{\partial x}\right\rangle_\eta\ . \tag{37}$$

Discretizing this equation and identifying $v_i(t)=v(x_i,t)$ with σ_i, one can see a term-by-term agreement between (33) and (34). This agreement, of course, does not prove the equivalence of the two models since (33) and (34) are only the first equations in the hierarchy of equations for the correlation functions. We can further argue for the equivalence, however, on the basis of universality. That is, it should be noted that our model contains the two distinguishing features of the field theoretic model (35): (i) the particles are deposited in the valleys and evaporate from the peaks which is essentially a surface tension driven relaxation process producing the $\partial^2 h/\partial x^2$ term in (35); (ii) for $p_+\neq\frac{1}{2}$ the surface moves with nonzero velocity and this nonzero velocity is responsible for the $(\partial h/\partial x)^2$ term in (35). We note that λ is proportional to the velocity of the interface.[14] A final point is that the conservation law of the kinetic Ising model ($\sum_i \sigma_i=0$) has its counterpart in the field theoretic model:

$$\int_0^L \frac{\partial h}{\partial x}dx=0$$

and no other obvious conservation laws exist.

Burgers's equation has been studied[14,17] by dynamic renormalization group methods. Three fixed points were found. The trivial one ($\nu^*\neq 0$, $\lambda^*=0$) describes the free-field scaling ($\eta=0$, $z=2$) which characterizes the equilibrium case ($p_+=\frac{1}{2}$) of our model. The nontrivial fixed point ($\nu^*\neq 0$, $\lambda^*\neq 0$) determines the scaling form for a moving interface ($\eta=0$, $z=\frac{3}{2}$). Since the trivial fixed point is unstable with respect to λ and since the third fixed point ($\nu^*=0$, $\lambda^*=0$, random deposition) cannot be reached in the parameter space of our model, we may expect that the nonequilibrium case ($p_+\neq\frac{1}{2}$) of our model is in one universality class with Burgers's equation for nonzero λ. This expectation is supported by the results of Monte Carlo simulations presented in the next section.

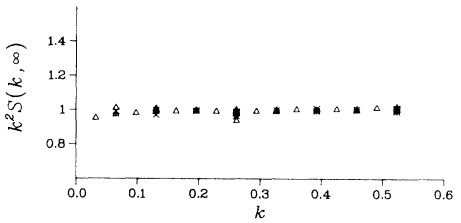

FIG. 2. Steady-state structure factor $S(k,\infty)$ multiplied by k^2 for the equilibrium ($\alpha=0$, denoted by $+$), full growth ($\alpha=1$: $\triangle$) and the intermediate growth ($\alpha=0.5$: $\times$) regime of model I. The data are obtained by growing $N=3000$ deposits for each strip width of $L=24$, 48, and 96 ($L=192$ has also been investigated for $\alpha=1$) and all the points with $k<\pi/6$ are displayed.

IV. COMPUTER SIMULATIONS

In this section the results of extensive Monte Carlo simulations which we have carried out for our model are reported. In the preceding section we conjectured that the evolution of the interface could be described in terms of two fixed points of the dynamic renormalization group equations of Kardar *et al.*[14] These recursion relations predict that for any nonzero α, $\eta=0$ and $z=\frac{3}{2}$, whereas for $\alpha=0$, $\eta=0$ and $z=2$. The exponent η can be determined from the steady-state ($t\to\infty$) limit of the structure factor $S(k,t)$. In Fig. 2 we display the function

TABLE I. The effective exponent $1/z_{\text{eff}}$ obtained by use of Eq. (39) for $t=L/12$ and $t=L/6$ for model I for $\alpha=0$, $\alpha=1.0$ and $\alpha=0.5$. The conjectured exponents correspond to $\eta=0$, $z=2$ for $\alpha=0$, and $\eta=0$, $z=1.5$ for $\alpha\neq 0$.

L	$\alpha=0$		$\alpha=1.0$		$\alpha=0.5$	
	$t=L/12$	$t=L/6$	$t=L/12$	$t=L/6$	$t=L/12$	$t=L/6$
24	0.58	0.60	0.65	0.79	0.62	0.69
48	0.56	0.60	0.70	0.76	0.60	0.66
96	0.54	0.57	0.70	0.74	0.60	0.64
192	0.53	0.55	0.69	0.71	0.60	0.63
384	0.52	0.52	0.69	0.71	0.62	0.65
768	0.52	0.52	0.68	0.69	0.62	0.66
1536	0.51	0.51	0.68	0.70	0.63	0.65
3072	0.52	0.52	0.70	0.71	0.66	0.68
Conjecture	0.50		$\frac{2}{3}$		$\frac{2}{3}$	

$k^2S(k,\infty)$ for three values of the parameter α (0,0.5,1.0) and for various lengths L. In all three cases the function $k^2S(k,\infty)$ seems to approach a finite nonzero limit as k approaches zero, indicating that η is zero or at least very small.

The exponent z can be determined from the stationary-state correlation function $\Phi(k,t)$ (5), from the relaxation function $\Psi(k,t)$ (6) or simply from the width $\xi^2(L,t)$ (2) for short times. If $z>1$ and $t\approx L$, the scaling form of $S(k,t)$ (7) yields

$$\xi^2(L,t)\sim t^{(1-\eta)/z}\sim L^{(1-\eta)/z} . \tag{38}$$

If one assumes that $\eta=0$ one can determine an effective dynamic exponent z_{eff} from the formula:

$$\frac{1}{z_{\text{eff}}(L)}=\frac{\ln[\xi^2(2t,2L)/\xi^2(t,L)]}{\ln(2)} , \tag{39}$$

where we must insure that $1\ll t\ll L^z$. In Table I we show the variation of the effective exponent at $t=L/12$ and $t=L/6$ as function of L for $\alpha=0$ (equilibrium growth), $\alpha=1.0$ and $\alpha=0.5$. For the smaller substrate lengths the data are the result of averaging ξ^2 over as many as 20 000 samples. For the largest substrates studied ($L=6144$) between 300 and 400 clusters were constructed.

The data of Table I are consistent with the conjecture (Sec. III) that $z=2$ for $\alpha=0$ and $z=\frac{3}{2}$ for $\alpha\neq 0$ and with the results of Meakin *et al.*[18] for $\alpha=1$. Moreover, for $\alpha=0$, we can compare the results of the simulations with the exact solution [Eq. (24)]. In all cases the values of ξ obtained from the simulations agree to within 1% with the exact solution. It is also noteworthy that the effective exponent still differs from the asymptotic value of 0.5 for substrate lengths as large as 3072. If one evaluates formula (39) using the exact solution (24) one finds that substrate lengths of order $L=50\,000$ are needed before $1/z_{\text{eff}}$ reaches the value of 0.50 to two significant figures. These finite-size effects are presumably due to the contributions to ξ from the nonscaling (large k) regions of the Brillouin zone and should be equally important for $\alpha\neq 0$. Nevertheless, Table I provides some evidence that the nontrivial fixed point of the Burgers's equation determines the behavior of the model for any nonzero value of α.

A more detailed and less ambiguous characterization of the interface is provided by the relaxation function $\Psi(k,t)$ [Eq. (7)] and by the stationary-state correlation function $\Phi(k,t)$ [Eq. (5)]. In Fig. 3 we display $\Psi(k,t)$ for the equilibrium growth case ($\alpha=0$) plotted as function of the scaled variable k^2t for $L=24$, 48, and 96 and several of the smallest k's. The data has collapsed quite precisely onto a single curve, indicating that the large finite-size effects apparent in Table I are absent here. Similar data is presented in Fig. 4 for the stationary-state correlation function $\Phi(k,t)$. Once again, a single universal function of the scaled variable k^2t describes the decay of fluctuations in the steady state for small k.

In Figs. 5 and 6 the same functions are plotted for $\alpha=1.0$ (maximum growth rate) as a function of the scaled variable k^zt with $z=1.55$. This value of z produces the best collapse of the data for both $\psi(k,t)$ and $\Phi(k,t)$, as judged by eye. The results for the relaxation function (Fig. 5) are for values of L up to 192, and, on the basis of this data one could quote the estimate $z=1.55\pm 0.1$ with confidence. The steady-state correlation function displays an effect which we have previously found[13] in the Eden model. The data separate into two branches; the upper branch corresponds to $k=2\pi/L$, the smallest nonzero value of k in the Brillouin zone; the lower branch corresponds to the remaining low-lying values of k. Both

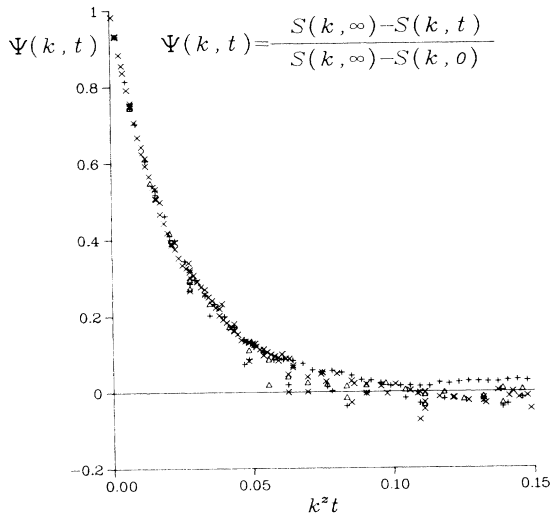

FIG. 3. Relaxation function $\Psi(k,t)$ [Eq. (6)] for the equilibrium growth ($\alpha=0$) regime of model I plotted as function of k^zt with $z=2$. Systems with $L=24$, △; 48, +; and 96, × are included and at least $N=3000$ clusters have been grown for each L. The data points are from the region $k<\pi/6$ of the Brillouin zone.

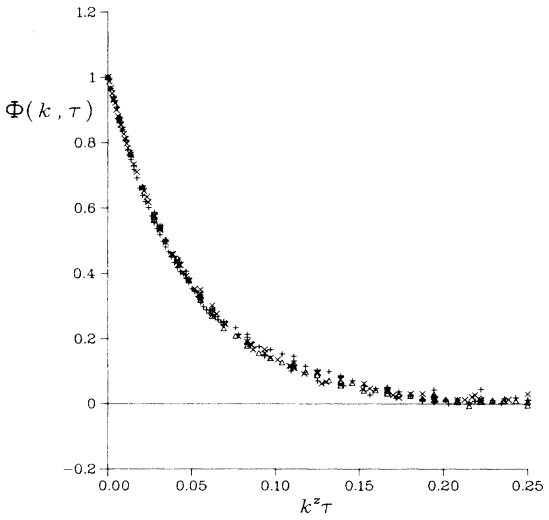

FIG. 4. The same as Fig. 3 but for the steady-state time-correlation function $\Phi(k,t)$ [Eq. (5)]. The dynamic critical exponent z is the same as in Fig. 3 ($z=2$).

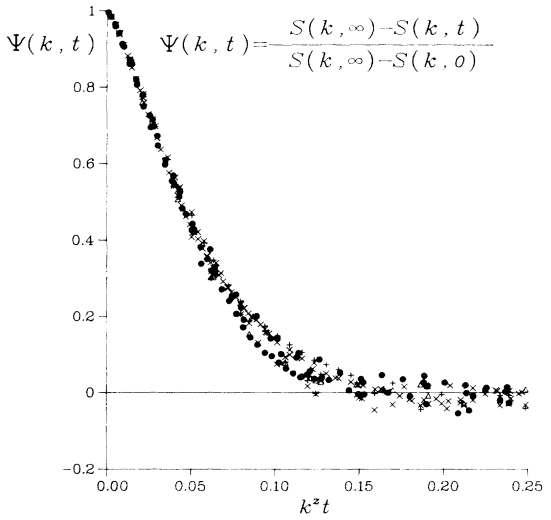

FIG. 5. Relaxation function $\Psi(k,t)$ for the full growth ($\alpha=1$) regime of model I plotted as function of $k^z t$ where $z=1.55$. Specifications are the same as for Fig. 3 except that the data are obtained from growing $N=6000$ deposits for each $L=24$, 48, and 96 and $N=3000$ deposits for $L=192$ (denoted by solid circles).

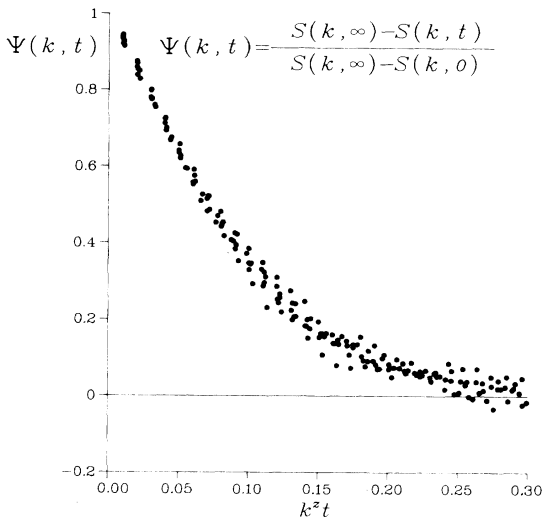

FIG. 7. Relaxation function $\Psi(k,t)$ for the intermediate growth ($\alpha=0.5$) regime of model I as function of $k^z t$ with $z=1.57$. The data is for a strip of width $L=768$ and the seven lowest values of k are included.

branches are reasonably well collapsed for a single value of z.

Finally we discuss the case of $\alpha=0.5$ which is intermediate between equilibrium and maximum growth. In this case we expect, on the basis of the dynamic renormalization group theory of the Burgers's equation[14,17] to see the effects of competition between the two fixed points. We have calculated the relaxation function $\Psi(k,t)$ for L up to 768. When one attempts to collapse the data onto a single curve, when plotted against $k^z t$, one finds that for a given L, a single effective exponent $z(L)$ produces well-converged data for the low-lying values of k corresponding to that particular L. The best convergence of the data occurs for $z(48)=1.85$, $z(96)=1.75$, $z(192)=1.70$, $z(384)=1.65$, and $z(768)=1.57$. We have plotted $\Psi(k,t)$ for $L=768$ as function of $k^z t$ with this value of z in Fig. 7. This data was obtained from only 800 samples and is quite noisy. There is, however, no systematic variation of the relaxation function with the magnitude of k. We therefore expect that more extensive simulations would produce a very well-converged single curve, as occurs for smaller substrate lengths, and, on the basis of the systematic decrease of $z(L)$ with increasing L, that the asymptotic value of $z=z(\infty)=1.5$.

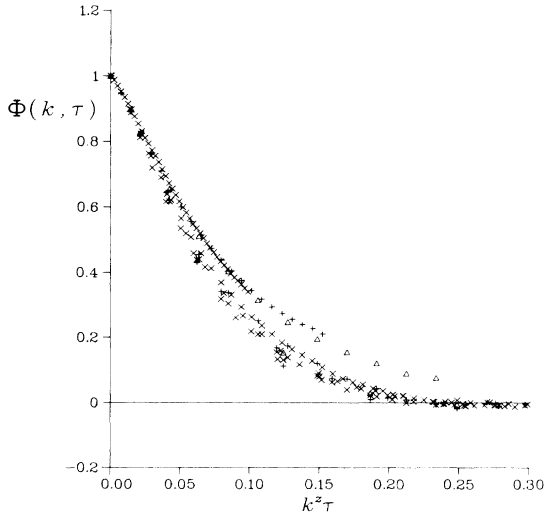

FIG. 6. Same as Fig. 5 but for the steady-state time-correlation function $\Phi(k,t)$ for strips of width $L=24$, 48, and 96.

Thus these simulations are entirely consistent with the notion that the dynamics of the model are describable in terms of the fixed points of Burgers's equation. Moreover the best estimates of the dynamic exponent are obtained from the relaxation function $\Psi(k,t)$ rather than from the width $\xi(L,t)$ of the active zone, as one would expect, since this function directly probes the scaling region.

Finally, one can qualitatively understand the two difference values of z in terms of the diffusion of particles in one dimension. As described in Sec. II, our model is equivalent to a hard-core lattice gas with the down spins representing particles, the up spins vacant sites. Deposition corresponds to a particle hopping to the right, evaporation to a particle hopping to the left. Thus, if $\alpha\neq 0$ there is a drift in the particle motion. In their investigation of diffusive systems van Beijeren *et al.*[19] found that in driven systems density fluctuations spread as $t^{2/3}$ whereas they spread as $t^{1/2}$ if there is no uniform drift. The time to reach the stationary state, $t_{\rm eq}$, can thus be crudely estimated by requiring that density fluctuations spread over a distance L. Thus $t_{\rm eq}\sim L^2\sim k^{-2}\sim k^{-z}$ with

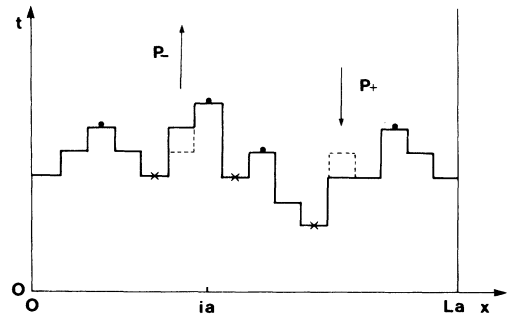

FIG. 8. Model II of interface evolution defined by deposition and evaporation events. Deposition (evaporation) occurs randomly at any site except at local maxima (minima) denoted by solid circles (crosses) where deposition (evaporation) is forbidden. The rate of deposition and evaporation is proportional to p_+ and $p_-=1-p_+$, respectively.

$z=2$ for the equilibrium case and $z=\frac{3}{2}$ for nonequilibrium growth, in agreement with our results.

V. UNIVERSALITY AND MODEL II

As discussed in the Introduction, the analogies with critical phenomena suggest that the exponents η and z are universal, i.e., they depend only on general features of the system such as the dimensionality, the symmetries of the steady state, and the symmetries of the equation of motion. The results of the preceding section are in accord with this expectation since the change in z from 2 to $\frac{3}{2}$ is accompanied by the breaking of time-reversal invariance.

In order to obtain further evidence for or against universality and to ascertain the role of time-reversal symmetry, we investigate, in this section, whether or not η and z are changed if the growth rules which define the motion of the interface are slightly modified.

The modified model (model II) is shown in Fig. 8. Particles (squares in $d=2$) are deposited with equal probability p_+ at any site except at local maximum of the surface at which deposition is forbidden. A particle which attempts to deposit at a local maximum is discarded. Evaporation occurs with probability $p_-=1-p_+$, again at any site on the surface except at the local minima.

The above rules imitate the effect of surface tension in the sense that they prevent the divergence of surface fluctuations for large time and furthermore, for $p_+\neq p_-$, we have a uniformly moving surface. Thus the physics is the same as in the case of model I introduced in Sec. II and one sees that going from $p_+=p_-$ ($\alpha=2p_+-1=0$) to $p_+1=p_-$ ($\alpha\neq 0$) breaks time-reversal symmetry. Consequently, considerations based on the notion of universality suggest that $\eta=0$ and $z=2$ for $\alpha=0$, while $\eta=0$ and $z=\frac{3}{2}$ for $\alpha\neq 0$.

TABLE II. Estimates of $(1-\eta)/2$ and $(1-\eta)/(2z)$ for model II in the zero velocity limit ($\alpha=0$). The width of the active zone in the stationary state $\xi(L,t=\infty)$ and in the nonequilibrium regime $\xi(L,t=L/4)$ is obtained from Monte Carlo simulations (1000 runs for each strip of width L). The error estimates are shown in parentheses in units of the last significant digit. The values of the critical exponents are obtained by assuming that $\xi(L,t=\infty)\sim L(1-\eta)/2$ and $\xi(L,t=L/4)\sim L(1-\eta)/(2z)$.

L	$\xi(L,t=\infty)$	$(1-\eta)/2$	$\xi(L,t=L/4)$	$(1-\eta)/(2z)$
4	1.26(2)		0.711(1)	
		0.86		0.47
8	2.29(3)		0.987(1)	
		0.63		0.45
16	3.54(4)		1.349(1)	
		0.56		0.38
32	5.22(6)		1.760(1)	
		0.51		0.37
64	7.44(8)		2.279(1)	
		0.50		0.34
128	10.5(3)		2.881(1)	
				0.31
256			3.571(1)	
				0.29
512			4.351(1)	
				0.28
1024			5.268(2)	
				0.27
2048			6.367(3)	
				0.27
4096			7.661(4)	
				0.26
8192			9.16(7)	
If $\eta=0$, $z=2$		0.50		0.25

The results of our Monte Carlo simulations for the case of $\alpha=0$ are shown in Table II, those for $\alpha=1$ are shown in Table III. We have assumed the scaling form (7) of $S(k,t)$ and calculated η and z by measuring the width of the active zone both in the stationary state $\xi(L,t\approx\infty)\sim L^{(1-\eta)/2}$ and at short times, $\xi(L,t=L/4)\sim L^{(1-\eta)/(2z)}$.

The data on the width in the stationary state suggest that as the system size is increased $\eta\to 0$ for both $\alpha=0$ and $\alpha\neq 0$. Since ξ contains contributions from the short wavelength modes it may, however, display strong finite-size effects. Thus the conclusion $\eta=0$, based on systems of size $L\leq 128$, should be viewed with some caution. It seems, however, that $\eta=0$ for any one-dimensional surface on which the proliferation of long wavelength modes (roughening) is not prevented by some long-range forces or effects. Since we do not see the present of such long-range forces in our model we made no special effort to determine η to high accuracy.

Once $\eta=0$ is taken for granted, z can be estimated from the short-time behavior of ξ. One can study systems with much larger L in this case since the evolution has to be followed only to times of order L instead of to $t\sim L^2$ or $t\sim L^{3/2}$ needed to reach the stationary state.

Although we expect finite-size effects to be large in ξ and, indeed, do not see complete convergence, the results shown in Tables II and III are consistent with the expectation that for $p_+=p_-$, $z=2$, and that $z=\frac{3}{2}$ for $p_+=1$, $p_-=0$. Thus we find support for the hypothesis that the breaking of time-reversal symmetry is the underlying cause for the change of the dynamic critical exponent z.

As is known from the theory of dynamic critical phenomena, z is sensitive to changes in the relevant symmetries of the equations of motion, i.e., to changes in the conservation laws of quantities which couple to the order parameter. Thus, when attempting to classify the various growth processes one should carefully check for the presence of conservation laws. For example, models I and II seem to be identical from the point of view of conservation laws. Closer examination shows, however, that this is not the case.

Using the particle interpretation of model I, one sees that the number of particles and the number of empty sites are conserved quantities. If one tries to construct a similar interpretation of model II, one must assign to the bond between sites i and $i+1$ $n_A^{(i)}=h_{i+1}-h_i$ particles of type A if $h_{i+1}>h_i$ or $n_B^{(i)}$ particles of type B if $h_{i+1}<h_i$. The evolution of the surface now corresponds to the hopping of these particles. In addition to the hopping motion, pairs of AB particles may be created at adjacent sites and neighboring pairs of AB particles may also annihilate each other.[21] Thus, neither the number of A- or B-type particles nor the number of empty sites are conserved quantities. The only conserved quantity is the difference between the number of type-A particles and type-B particles:

$$\sum_i (n_A^{(i)}-n_B^{(i)})=0 .$$

TABLE III. Same as Table II but for the full growth limit ($\alpha=1$) of model II.

L	$\xi(L,t=\infty)$	$(1-\eta)/2$	$\xi(L,t=L/4)$	$(1-\eta)/(2z)$
4	1.88(1)		0.68(1)	
		0.74		0.56
8	3.15(1)		1.00(1)	
		0.58		0.51
16	4.71(2)		1.42(1)	
		0.51		0.45
32	6.70(3)		1.94(1)	
		0.50		0.41
64	9.48(4)		2.57(1)	
		0.52		0.37
128	13.6(2)		3.32(1)	
				0.34
256			4.21(1)	
				0.31
512			5.23(1)	
				0.30
1024			6.44(2)	
				0.30
2048			7.91(2)	
				0.30
4096			9.72(3)	
				0.30
8192			11.99(2)	
If $\eta=0$, $z=\frac{3}{2}$		0.50		$\frac{1}{3}$

The above differences notwithstanding, models I and II seem to have the same dynamic exponent. The irrelevance of these "hidden" conservation laws is not obvious, however, as evidenced by Family's recent results[22] on a simple two-dimensional model of deposition. In this model the effect of surface tension is taken into account by defining the evolution of the surface through the following rule: three neighboring columns are chosen at random and the next particle is added to the column with the smallest height. This model seems to be closely related to the $p_+ = 1$, $p_- = 0$ limit of our model II. Nevertheless, Family finds $z = 2$, indicating that some of the "hidden" conservation laws are relevant in his case. Clearly, more detailed studies are needed in order to clarify the relevant parameters in the classification of surface-evolution processes.

ACKNOWLEDGMENT

This research was supported by the Natural Sciences and Engineering Research Council of Canada.

*Permanent address: Institute for Theoretical Physics, Eötvös University, H-1088 Budapest, Hungary.

[1]*Kinetics of Aggregation and Gelation*, edited by F. Family and D. P. Landau (North-Holland, Amsterdam, 1984).

[2]*On Growth and Forms: Fractal and Non-Fractal Patterns is Physics*, edited by H. E. Stanley and N. Ostrowsky (Nijhoff, Boston, 1986).

[3]*Fractals in Physics*, edited by L. Pietronero and E. Tosatti (North-Holland, Amsterdam, 1986).

[4]T. A. Witten and L. M. Sander, Phys. Rev. Lett. **47**, 1400 (1982).

[5]T. C. Halsey, M. H. Jensen, L. P. Kadanoff, I. Procaccia, and B. I. Shraiman, Phys. Rev. A **33**, 1141 (1986); A. Coniglio, *Fractals in Physics*, Ref. 3, p. 165.

[6]M. Plischke and Z. Rácz, Phys. Rev. Lett. **53**, 415 (1984).

[7]T. C. Halsey, P. Meakin, and I. Procaccia, Phys. Rev. Lett. **56**, 854 (1986).

[8]P. Meakin (unpublished).

[9]M. Eden, *Proceedings of the Fourth Berkeley Symposium on Mathematics, Statistics, and Probability*, edited by F. Neyman (University of California Press, Berkeley, 1961), Vol. 4, p. 223.

[10]M. J. Vold, J. Colloid Sci. **14**, 68 (1959); J. Phys. Chem. **63**, 1608 (1959).

[11]F. Family and T. Vicsek, J. Phys. A **18**, L75 (1985).

[12]R. Jullien and R. Botet, J. Phys. A **18**, 2279 (1985).

[13]M. Plischke and Z. Rácz, Phys. Rev. A **32**, 3825 (1985).

[14]M. Kardar, G. Parisi, and Y. C. Zhang, Phys. Rev. Lett. **56**, 889 (1986).

[15]S. F. Edwards and D. R. Wilkinson, Proc. R. Soc. London, Ser. A **381**, 17 (1982).

[16]J. M. Burgers, *The Nonlinear Diffusion Equation* (Riedel, Boston, 1974).

[17]D. Forster, D. R. Nelson, and M. J. Stephen, Phys. Rev. A **16**, 732 (1977).

[18]P. Meakin, L. M. Sander, and R. Ball (unpublished).

[19]H. van Beijeren, R. Kutner, and H. Spohn, Phys. Rev. Lett. **54**, 2026 (1985).

[20]R. J. Glauber, J. Math. Phys. **4**, 294 (1963).

[21]This type of model has recently been considered in K. Kang and S. Redner, Phys. Rev. A **32**, 435 (1985).

[22]F. Family, J. Phys. A **20**, L441 (1986).